

UCLA

UCLA Previously Published Works

Title

Prediction of visual field progression with serial optic disc photographs using deep learning.

Permalink

<https://escholarship.org/uc/item/5q81x0xc>

Journal

British Journal of Ophthalmology, 108(8)

Authors

Mohammadzadeh, Vahid

Wu, Sean

Davis, Tyler

et al.

Publication Date

2024-07-23

DOI

10.1136/bjo-2023-324277

Peer reviewed



HHS Public Access

Author manuscript

Br J Ophthalmol. Author manuscript; available in PMC 2024 July 24.

Published in final edited form as:

Br J Ophthalmol. ; 108(8): 1107–1113. doi:10.1136/bjo-2023-324277.

Prediction of Visual Field Progression with Serial Optic Disc Photographs Using Deep Learning

Vahid Mohammadzadeh, MD¹, Sean Wu, BS², Tyler Davis, PhD³, Arvind Vepa, PhD³, Esteban Morales, MS¹, Sajad Besharati, MD¹, Kiumars Edalati, BS¹, Jack Martinyan, BS¹, Mahshad Rafiee, BS¹, Arthur Martinyan, BS¹, Fabien Scalzo, PhD^{2,3}, Joseph Caprioli, MD¹, Kouros Nouri-Mahdavi, MD, MS¹

¹Glaucoma Division, Stein Eye Institute, David Geffen School of Medicine, University of California Los Angeles, Los Angeles, California

²Department of Computer Science, Pepperdine University, Malibu, California

³Department of Computer Science, University of California Los Angeles, Los Angeles, California

Abstract

Aim: We tested the hypothesis that visual field (VF) progression can be predicted with a deep learning model based on longitudinal pairs of optic disc photographs (ODP) acquired at earlier time points during follow-up.

Methods: 3,919 eyes (2,259 patients) with 2 ODPs at least 2 years apart, and 5 24–2 visual field exams spanning 3 years of follow-up were included. Serial VF mean deviation (MD) rates of change were estimated starting at the 5th visit and subsequently by adding visits until final visit. VF progression was defined as a statistically significant negative slope at two consecutive visits and final visit. We built a twin-neural network with ResNet50-backbone. A pair of ODPs acquired up to a year before the VF progression date or the last VF in non-progressing eyes were included as input. Primary outcome measures were area under the ROC curve (AUC) and model accuracy.

Corresponding author: Kouros Nouri-Mahdavi, MD, MS, 100 Stein Plaza, Los Angeles, CA, 90095, USA, Phone: 310-794-1487, Fax: 310-794-6616, nouri-mahdavi@jsei.ucla.edu.

Contributors: **VM:** Involved in design and conduct of study, Data collection, Analysis and interpretation of data, Writing, Critical revision, Approval of the manuscript, **SW:** Involved in design and conduct of study, Analysis and interpretation of data, Writing, Critical revision, **TD:** Involved in design and conduct of study, Analysis and interpretation of data, Writing, Critical revision, **AV:** Involved in design and conduct of study, Writing, Critical revision, **EM:** Data collection, Writing, **SB:** Data collection, Writing, **KE:** Data collection, Writing, **JM:** Data collection, Writing, **MR:** Data collection, Writing, **AM:** Data collection, Writing, **FS:** Involved in design and conduct of study, Analysis and interpretation of data, Writing, Critical revision, Approval of the manuscript, **JC:** Involved in design and conduct of study, Analysis and interpretation of data, Writing, Critical revision, Approval of the manuscript, **KNM:** Involved in design and conduct of study, Data collection, Analysis and interpretation of data, Writing, Critical revision, Approval of the manuscript, Guarantor of work

Presented as a paper at the Annual Meeting of the American Glaucoma Society, March 2-5, 2023 (Austin TX)

Commercial Disclosures: None of the authors has any conflicts to disclose.

Disclaimer: The funding organizations had no role in the design or conduct of this research.

Competing interests: none declared.

Patient consent for publication: Not applicable.

Ethics approval: This study involves human participants and was approved by The University of California Los Angeles Institutional Review Board (IRB#19-000953). All protocols and the methods described adhered to the tenets of the Declaration of Helsinki. Participants gave informed consent to participate in the study before taking part.

Results: The average (SD) follow-up time and baseline VF MD were 8.1 (4.8) years and -3.3 (4.9) dB, respectively. VF progression was identified in 761 eyes (19%). The median (IQR) time to progression in progressing eyes was 7.3 (4.5–11.1) years. The AUC and accuracy for predicting VF progression were 0.862 (0.812–0.913) and 80.0% (73.9%–84.6%). When only fast-progressing eyes were considered (MD rate <-1.0 dB/year), AUC increased to 0.926 (0.857–0.994).

Conclusions: A deep-learning model can predict subsequent glaucoma progression from longitudinal ODPs with clinically relevant accuracy. This model may be implemented, after validation, for predicting glaucoma progression in the clinical setting.

Keywords

Glaucoma; progression; optic disc photographs; deep learning; Convolutional Neural Networks; visual fields; prediction

Introduction

Timely detection of disease progression is an unmet need for the management of glaucoma so that appropriate remedial action can be taken, and further visual loss is prevented. Various functional and structural modalities have been utilized for this task including visual field (VF) examination, optic disc photography (ODP), and optical coherence tomography. [1–3] Visual field testing remains the standard of care for functional evaluation in glaucoma. [4] Estimating VF rates of change is a practical and commonly used approach for identifying the speed of disease deterioration in glaucoma eyes and for detecting eyes with rapid progression. [5,6]

Optic disc photography is still commonly used for monitoring structural damage in glaucoma. It is widely available and does not require sophisticated software for visualization. Serial ODP is an established method to detect progressive glaucomatous damage especially in early to moderately severe stages of the disease. [7,8] Review and comparison of serial ODPs is laborious and specialized. Also, detection of change over time is subjective and there is high inter-rater variability even among glaucoma specialists. [9,10] Hence, ODP remains underutilized in the care of glaucoma patients.

Artificial intelligence (AI) methods are increasingly used in ophthalmology, especially in glaucoma. [11–13] A few studies have explored the performance of deep learning (DL) models for detection of glaucoma progression. [14–16] Medeiros and collaborators showed that circumpapillary retinal nerve fiber layer rates of change could be predicted with serial ODP. [17] Since functional visual deterioration is ultimately what matters to the patient when the disease progresses, [18,19] it is crucial to be able to design and implement DL models to predict future functional loss. The purpose of this study was to design a DL model to forecast future VF worsening relying on prior longitudinal ODPs available a year or longer before VF progression is detected.

Methods

Patients from Stein Eye Institute's clinical database were included in this study. The study was approved by the University of California Los Angeles's Institutional Review Board (IRB#19-000953), which waived the requirement for informed consent and adhered to the Declaration of Helsinki and the Health Insurance Portability and Accountability Act policies. The findings were reported according to the Strengthening of The Reporting of Observational Studies in Epidemiology (STROBE) statement checklist.

Participants were required to have 2 or more ODPs on separate visits at least 2 years apart and 5 visual field tests with 3 years of follow-up. We included all the VF tests that were acquired between one year before the baseline ODP date and one year after the final ODP date. The study participants had a diagnosis of primary open-angle glaucoma (POAG), normal tension glaucoma, pigmentary glaucoma, pseudoexfoliative glaucoma, or primary angle closure glaucoma (PACG).

Data collection

Disc photographs were acquired with two different devices: the Zeiss 450 Fundus Camera and the Zeiss FF 450 plus Fundus Camera with VISUPAC™ Digital Imaging System (both from Carl Zeiss Meditec, Dublin, CA). Conventional ODPs in 36mm slide format acquired before 2013 were digitized at a resolution of 2800×4200 pixels. Image quality was reviewed manually and low-quality blurred images or those with inadequate illumination were excluded (156 images, 2%).

The 24–2 VFs were acquired with Humphrey Field Analyzer II (Carl Zeiss Meditec, Dublin, CA) with the standard Swedish Interactive Thresholding Algorithm. Visual fields with false positive rates 15% were excluded. Data were exported as XML files to a personal computer.

Definition of visual field progression

We defined functional glaucoma progression based on rates of change of VF mean deviation (MD) with univariate linear regression of MD against time. For each study participant, multiple regressions were carried out starting with the first 5 visits; MD rates of change were re-estimated after sequentially adding additional visits until the last available VF. Hence each eye had a series of $n - 4$ estimates of MD rates of change (n = total number of VFs available during follow-up for each eye). For each iteration of MD regression analysis against time, a negative MD slope (i.e., slope <0 dB/year) with a p-value <0.05 was considered significant. The entire series of VFs in each eye was considered to be deteriorating if there were two consecutive statistically significant negative MD slopes within the series on the condition that the MD slope for the entire follow-up was also significantly negative. The time to glaucoma progression (time to event) was considered as the time interval between the baseline VF and the first detected significantly negative MD slope. The same approach was used for the definition of moderate and fast progression; eyes with significant MD rates <-0.5 dB/year and <-1.0 dB/year, respectively, were considered as moderate and fast progressors.

Deep learning model input

The DL model was trained from pairs of ODP images used as input and associated with an output representing the functional glaucoma progression. The first input image was the baseline and the second was the ODP acquired a year or more before VF progression in the progressing group and before the final VF exam in the stable group. Each ODP was randomly selected from the stereoscopic pair available. The cohort was split to create the training, validation, and testing datasets with an 80%/10%/10% proportion.

The deep learning approach

A twin-structured convolutional neural network (CNN) was used for predicting glaucoma progression utilizing pairs of baseline and final ODPs. The model consists of two copies of the same ResNet50 backbone, with shared weights between them, and a classification head. First, both inputs are passed through the backbone generating intermediate features that are subsequently concatenated and processed by the classification head to generate a final output.

The twin CNN ResNet50 backbone is pre-trained on ImageNet. This approach is known as transfer learning; it has been shown to be an efficient approach for evaluating images. Because ResNet50 is pre-trained on images sized $224 \times 224 \times 3$ pixels, we also resized our input images to $224 \times 224 \times 3$ pixels with bilinear interpolation. Our model accepts baseline and final images and passes each individually through the ResNet50 backbone. The extracted features are then globally pooled to reduce the channel dimensionality to 1 and then passed through a batch normalization layer before they are concatenated together (Supplemental Figure 1). We used a two-phase transfer learning approach by only training the final layer in the first phase to prevent weight destruction. The convolutional ResNet weights were fine-tuned once performance was stabilized. In order to determine the optimal hyperparameters for our model, we manually performed a random search over 20 different combinations of phase one and phase two learning rates, dropout rates, layers for model freezing, and the hidden dimension for the final connected layer.

The metric optimized during the random search was area under the receiver operating characteristic curve (AUC) in the validation set. All models were trained using Adam optimizer, a batch size of 32, and binary cross entropy loss for 1 epoch in phase one and 60 epochs in phase two. To account for the uneven distribution of progressing and stable eyes in the dataset, the loss weight for the progressing eyes was increased.

In the final step, we applied augmentations to the ODPs during training in order to reduce the likelihood of overfitting. Augmentations applied included random rotations of up to 273 degrees [20] clockwise or counterclockwise, a random vertical or horizontal shift of up to 15%, a random contrast change 20%, and a random zoom 15%. To enhance the generalizability of our model on external data regardless of the position and rotation, individual augmentations were applied to each image including those from the same eye.

The model was trained for glaucoma progression criteria as detailed above and for moderate and fast-progressing eyes. The model was developed with Python 3.9.7 libraries including TensorFlow 2.9.0, Keras Tuner 1.04, NumPy 1.19.5, SciPy 1.7.1, and scikit-learn 0.24.2.

Assessing model performance

We estimated AUCs to assess performance of the model for predicting functional glaucoma progression in the testing dataset. We also calculated partial AUCs (pAUC) at specificities higher than 90%. Sensitivity, specificity, and accuracy were calculated from confusion matrices with a threshold of 0.5. Bootstrapping was carried out 5000 times was performed to provide the 95% confidence interval (CI). In order to determine whether the model is relying on clinically expected features for predicting glaucoma progression, we generated saliency maps with eXplanation with Ranked Area Integrals (XRAI). [21] We considered the baseline image constant for generating the XRAI saliency maps and the XRAI map highlighted the most important features corresponding to the final image. Finally, we overlaid the top 30% of the features onto the final ODP (the second of the pair) to visualize regions on the final ODP where those features were mapped.

Results

A total of 3,919 eyes (2,259 patients) were included in this study. Seven hundred and sixty-one eyes (19.0%) demonstrated VF progression when a significant MD rate was described as MD slope <0 dB/year. Based on the more stringent stricter criteria, i.e., MD slopes <-0.5 and <-1.0 dB/year, 347 (9%) and 93 (2%) of eyes showed progression. The mean (SD) timeline between the final ODP and the time to detect progression for the progressing eyes was 1.7 (1.8) years. The mean (SD) follow-up time and baseline VF MD for the stable and progressing eyes were 7.6 (4.7) and 10.3 (4.9) years ($p < .001$) and -3.3 (4.9) and -3.6 (4.8) dB ($p = .19$), respectively (Table 1).

Performance of the DL model for predicting glaucoma progression is displayed in Table 2. For the least stringent criteria, the AUC (95% CI) for predicting functional glaucoma progression was 0.862 (0.812–0.913). The corresponding sensitivity, specificity, and accuracy (95% CI) were 83.0% (73.4%–91.4%), 78.5% (68.8%–86.6%), and 80.0% (73.9%–84.6%), respectively. We further stratified the eyes in the testing dataset as mild-stage glaucoma (baseline MD >-6 dB) and moderate to advanced-stage glaucoma (baseline MD ≤ -6 dB). The AUC for predicting future glaucoma progression for the two subgroups was 0.856 (0.797–0.915) and 0.860 (0.751–0.968), respectively.

For the moderate-progressing eyes, the corresponding AUC (95% CI) for predicting subsequent VF progression was 0.890 (0.845–0.935) with corresponding sensitivity, specificity, and accuracy of 93% (77%–100%), 77% (65%–88%), and 79% (68%–88%) (Table 2). In addition, for the fast-progressing eyes, the corresponding AUC, sensitivity, specificity, and accuracy (95% CI) were 0.926 (0.857–0.994), 100% (77.7%–100%), 80% (67.9%–97.8%) and 80.4% (68.6%–97.4%), respectively (Table 2). However, the AUC difference between the three criteria was not statistically significant ($p > 0.141$). Figure 1 demonstrates the receiver operating characteristics curves for the model's performance for MD rates <0 dB/year, <-0.5 dB/year, and <-1.0 dB/year criteria. The partial AUC at 90% specificity for models using MD rates <0 dB/year, <-0.5 dB/year, and <-1 dB/year criteria were 0.040 (0.027–0.054), 0.036 (0.021–0.052) and 0.058 (0.030–0.085), respectively (Figure 2). The pairwise pAUC differences for the 3 models were not statistically significant ($p > .18$ for all).

Figure 3 provides the saliency maps based on the XRAI approach for two eyes that were correctly labeled as progressing and one eye that was correctly labeled as stable with our DL model. The first progressing eye (Figure 3A) demonstrated generalized rim loss on the final disc photograph compared to the baseline ODP; the highest attention was concentrated on the entire rim on the XRAI map (third column). In the second progressing eye (Figure 3B), the development of inferior (and superior) notching on the final photographs can be observed; the XRAI map mostly focused on the inferior rim area for making the prediction. However, in the stable eye (Figure 3C), the overall attention intensity is low across the region of interest on the XRAI map.

Discussion

We designed a deep learning model for predicting subsequent functional glaucoma progression one or more years after the last available optic disc photograph in eyes with longitudinal series of ODPs in a retrospective cohort with an average 8-year follow-up period. The AUC for predicting glaucoma progression was 0.862 (95% CI: 0.812, 0.913). When we considered more stringent criteria for defining functional glaucoma progression, the DL model demonstrated a higher AUC (0.890 and 0.926) although the differences were not statistically significant. The overall accuracy was about 80% (79.0–80.4%) regardless of the criteria used to define progression. While the accuracy may seem suboptimal, a review of the literature shows that no major available prognostic algorithm proposed for forecasting the development or progression of glaucoma has achieved this level of accuracy. [22, 23] The proposed model could be used in the clinical setting to provide clinicians managing glaucoma with a progression probability index and could help preserve functional status in glaucoma patients.

Assessing visual field deterioration over time is crucial and remains the standard of care for detecting glaucoma progression as it is associated with decreased quality of life. [24] A substantial amount of structural loss may take place before VF changes can be identified. [25,26] Therefore if a DL model is able to predict future VF progression, it could help prevent further functional deterioration and maintain patients' quality of life. We trained the DL model merely with baseline and follow-up pairs of ODPs acquired one or more years before the first identifiable evidence of VF progression or the final VF in stable patients. There is evidence indicating that progressive retinal nerve fiber layer and neuroretinal rim thinning could occur up to several years before VF deterioration can be detected. [27] Therefore, we hypothesized that a DL model trained with a large dataset of longitudinal ODPs could be beneficial in predicting future functional deterioration, addressing the high inter-observer variability among clinicians when grading serial ODPs. [10,28] Our findings suggest that the performance of the twin CNN model used in the current study was clinically relevant for detection of future functional deterioration.

In the current dataset, most of the baseline ODPs were digitized scans whereas the second ODP pair was mainly acquired digitally. Therefore, there might have been potential differences in image quality between the baseline and final images. Our model was able to handle this difference in quality, identify important landmarks between the baseline and final images and determine their areas of similarity or differences. It is plausible that if

the baseline and final ODPs are acquired in the exact same manner, model performance might improve. The high values of AUC and other performance metrics along with the observed characteristics of the saliency maps strongly suggest that the DL model is focusing its 'attention' on the relevant areas of the optic disc region. The saliency maps (developed by XRAI) showed that the model had mostly considered changes in the optic nerve rim (generalized or focal) in order to learn whether a specific eye was progressing or not (Figure 3).

Some previous studies explored prediction of glaucoma development or progression with clinical and demographic factors. [22,23,29] The Ocular Hypertension Treatment Study (OHTS) predictive model was used to assess progression to glaucoma in the European Glaucoma Progression Study (EGPS) cohort. Using age, intraocular pressure, vertical cup-to-disc ratio, VF pattern standard deviation at baseline, and central corneal thickness, the resulting C-statistic, a performance metric similar to AUC, was 0.74. [22] In a subsequent study, adding long-term intraocular pressure variability to the baseline predictors did not enhance the performance of the predictive model. [30] Another study validated the OHTS-EGPS predictive model on four different cohorts (the highest sample size was 393). [31] The C-index for the four different cohorts ranged between 0.69 and 0.83. In our study, despite using only a pair of longitudinal ODPs for predicting future glaucoma progression, the resulting AUC was clinically relevant (AUC =0.862). We did not put any demographic data into the DL model; one would expect that the performance of the would likely increase with additional demographic and clinical information. When performance of the model was compared in mild vs. moderate to advanced stage glaucoma eyes, the DL model demonstrated equal performance for predicting future functional glaucoma progression. One important finding was the trend toward a better performance of the model for predicting glaucoma progression in moderate or fast-progressing eyes. The AUC for predicting glaucoma progression for MD rates <0 dB/year was 0.862, whereas it was 0.890 for MD rates <-0.5 dB/year and 0.926 for MD rates <-1.0 dB/year. When we considered the most clinically relevant parts of the ROC curves where the specificity is greater than 90%, the partial-AUCs were higher for the fast and moderately-progressing eyes. Fast-progressing glaucoma eyes require more aggressive management since they are at higher functional deterioration risk and worsening quality of life. [32] The current model would be helpful in the clinical setting for detecting fast-progressing eyes and could assist clinicians with intensifying treatment of glaucoma when indicated. This could be especially of value in low-tech environments where a fundus camera might be the only imaging modality available. It would be interesting to investigate if the performance of these models differs depending on the patient's ethnicity, particularly for those of African or Hispanic descent, who are at higher risk of glaucoma progression. [33,34]

A limitation of our study is that we used global VF rates of change (MD rates) for detecting glaucoma progression. It is possible that DL models incorporating pointwise linear regression or other models could perform better for detection of functional glaucoma progression. A recent study by Medeiros et al., however, showed that MD rates were strong predictors of glaucoma progression and could be used as valid endpoints in clinical research. [35] In the ODP dataset, both right and left stereo images were available. Although there are

slight differences between these images, we randomly selected one out of the two. There is no a priori reason that this might have affected the results.

In conclusion, we demonstrate that a proposed deep-learning model with longitudinal pairs of optic disc photographs is able to predict future functional glaucoma progression at least one year ahead of the event with relevant clinical accuracy. The performance of the model might be better for fast-progressing glaucoma patients. This model could be used in clinical and research settings to identify glaucoma patients at higher risk of disease deterioration once proper validations have been carried out.

Supplementary Material

Refer to Web version on PubMed Central for supplementary material.

Acknowledgment

Funding:

This work was supported by an NIH R01 grant (R01-EY029792, KNM) and an unrestricted Departmental Grant from Research to Prevent Blindness.

Data availability statement:

The datasets generated and/or analyzed during the current study are available from the corresponding author upon reasonable request.

References

1. Quigley HA, Katz J, Derick RJ, Gilbert D, Sommer A. An evaluation of optic disc and nerve fiber layer examinations in monitoring progression of early glaucoma damage. *Ophthalmology* 1992;99(1):19–28. [PubMed: 1741133]
2. Rabiolo A, Morales E, Mohamed L, et al. Comparison of Methods to Detect and Measure Glaucomatous Visual Field Progression. *Transl Vis Sci Technol* 2019;8(5):2.
3. Mohammadzadeh V, Fatehi N, Yarmohammadi A, et al. Macular Imaging with Optical Coherence Tomography in Glaucoma. *Surv Ophthalmol* 2020.
4. Caprioli J The importance of rates in glaucoma. *American Journal of Ophthalmology* 2008;145(2):191–192. [PubMed: 18222187]
5. Caprioli J, Mock D, Bitrian E, et al. A method to measure and predict rates of regional visual field decay in glaucoma. *Invest Ophthalmol Vis Sci* 2011;52(7):4765–4773. [PubMed: 21467178]
6. Heijl A, Leske MC, Bengtsson B, Bengtsson B, Hussein M, Early Manifest Glaucoma Trial G. Measuring visual field progression in the Early Manifest Glaucoma Trial. *Acta Ophthalmol Scand* 2003;81(3):286–293. [PubMed: 12780410]
7. Ohnell H, Heijl A, Anderson H, Bengtsson B. Detection of glaucoma progression by perimetry and optic disc photography at different stages of the disease: results from the Early Manifest Glaucoma Trial. *Acta Ophthalmol* 2017;95(3):281–287. [PubMed: 27778463]
8. Amini N, Alizadeh R, Parivissutt N, Kim E, Nouri-Mahdavi K, Caprioli J. Optic Disc Image Subtraction as an Aid to Detect Glaucoma Progression. *Translational Vision Science & Technology* 2017;6(5):14.
9. Breusegem C, Fieuws S, Stalmans I, Zeyen T. Agreement and accuracy of non-expert ophthalmologists in assessing glaucomatous changes in serial stereo optic disc photographs. *Ophthalmology* 2011;118(4):742–746. [PubMed: 21055815]

10. Jampel HD, Friedman D, Quigley H, et al. Agreement among glaucoma specialists in assessing progressive disc changes from photographs in open-angle glaucoma patients. *American Journal of Ophthalmology* 2009;147(1):39–44.e31. [PubMed: 18790472]
11. Asaoka R, Murata H, Hirasawa K, et al. Using Deep Learning and Transfer Learning to Accurately Diagnose Early-Onset Glaucoma From Macular Optical Coherence Tomography Images. *Am J Ophthalmol* 2019;198:136–145. [PubMed: 30316669]
12. Thompson AC, Jammal AA, Berchuck SI, Mariottoni EB, Medeiros FA. Assessment of a Segmentation-Free Deep Learning Algorithm for Diagnosing Glaucoma From Optical Coherence Tomography Scans. *JAMA Ophthalmology* 2020.
13. Christopher M, Nakahara K, Bowd C, et al. Effects of study population, labeling and training on glaucoma detection using deep learning algorithms. *Translational Vision Science & Technology* 2020;9(2):27–27.
14. Dixit A, Yohannan J, Boland MV. Assessing Glaucoma Progression Using Machine Learning Trained on Longitudinal Visual Field and Clinical Data. *Ophthalmology* 2021;128(7):1016–1026. [PubMed: 33359887]
15. Medeiros FA, Jammal AA, Mariottoni EB. Detection of Progressive Glaucomatous Optic Nerve Damage on Fundus Photographs with Deep Learning. *Ophthalmology* 2020.
16. Hassan ON, SS, Mohammadzadeh V, et al.. Conditional GAN for Prediction of Glaucoma Progression with Macular Optical Coherence Tomography. In *International Symposium on Visual Computing Springer, Cham.* 2020 Oct 5.:761–772.
17. Medeiros FA, Jammal AA, Mariottoni EB. Detection of progressive glaucomatous optic nerve damage on fundus photographs with deep learning. *Ophthalmology* 2021;128(3):383–392. [PubMed: 32735906]
18. Ramulu PY, Hochberg C, Maul EA, Chan ES, Ferrucci L, Friedman DS. Glaucomatous visual field loss associated with less travel from home. *Optometry and Vision Science: official publication of the American Academy of Optometry* 2014;91(2):187. [PubMed: 24374635]
19. Medeiros FA, Gracitelli CP, Boer ER, Weinreb RN, Zangwill LM, Rosen PN. Longitudinal changes in quality of life and rates of progressive visual field loss in glaucoma patients. *Ophthalmology* 2015;122(2):293–301. [PubMed: 25444345]
20. Liu J, Chao F, Lin CM. Task augmentation by rotating for meta-learning arXiv 2020. arXiv preprint arXiv:2003.00804. 2003.
21. Kaphishnikov A, Bolukbasi T, Viégas F, Terry M. Xrai: Better attributions through regions. Paper presented at: Proceedings of the IEEE/CVF International Conference on Computer Vision 2019
22. Gordon MO, Torri V, Miglior S, et al. Validated prediction model for the development of primary open-angle glaucoma in individuals with ocular hypertension. *Ophthalmology* 2007;114(1):10–19. [PubMed: 17095090]
23. Medeiros FA, Weinreb RN, Sample PA, et al. Validation of a predictive model to estimate the risk of conversion from ocular hypertension to glaucoma. *Archives of Ophthalmology* 2005;123(10):1351–1360. [PubMed: 16219726]
24. Rulli E, Quaranta L, Riva I, et al. Visual field loss and vision-related quality of life in the Italian Primary Open Angle Glaucoma Study. *Scientific Reports* 2018;8(1):1–12. [PubMed: 29311619]
25. Hood DC, Kardon RH. A framework for comparing structural and functional measures of glaucomatous damage. *Prog Retin Eye Res* 2007;26(6):688–710. [PubMed: 17889587]
26. Medeiros FA, Zangwill LM, Bowd C, Mansouri K, Weinreb RN. The structure and function relationship in glaucoma: implications for detection of progression and measurement of rates of change. *Invest Ophthalmol Vis Sci* 2012;53(11):6939–6946. [PubMed: 22893677]
27. Pederson JE, Anderson DR. The mode of progressive disc cupping in ocular hypertension and glaucoma. *Archives of Ophthalmology* 1980;98(3):490–495. [PubMed: 7362506]
28. Varma R, Steinmann WC, Scott IU. Expert Agreement in Evaluating the Optic Disc for Glaucoma. *Ophthalmology* 1992;99(2):215–221. [PubMed: 1553210]
29. De Moraes CGV, Juthani VJ, Liebmann JM, et al. Risk factors for visual field progression in treated glaucoma. *Archives of Ophthalmology* 2011;129(5):562–568. [PubMed: 21555607]

30. Gordon MO, Gao F, Huecker JB, et al. Evaluation of a Primary Open-Angle Glaucoma Prediction Model Using Long-term Intraocular Pressure Variability Data: A Secondary Analysis of 2 Randomized Clinical Trials. *JAMA Ophthalmology* 2020;138(7):780–788. [PubMed: 32496526]
31. Takwoingi Y, Botello AP, Burr JM, et al. External validation of the OHTS-EGPS model for predicting the 5-year risk of open-angle glaucoma in ocular hypertensives. *British Journal of Ophthalmology* 2014;98(3):309–314. [PubMed: 24357494]
32. Anderson AJ, Chaurasia AK, Sharma A, et al. Comparison of rates of fast and catastrophic visual field loss in three glaucoma subtypes. *Invest Ophthalmol Vis Sci* 2019;60(1):161–167. [PubMed: 30640968]
33. Leske MC, Connell AM, Schachat AP, Hyman L. The Barbados Eye Study. Prevalence of open angle glaucoma. *Arch Ophthalmol* 1994;112(6):821–829. [PubMed: 8002842]
34. Buhrmann RR, Quigley HA, Barron Y, West SK, Oliva MS, Mmbaga BB. Prevalence of glaucoma in a rural East African population. *Invest Ophthalmol Vis Sci* 2000;41(1):40–48. [PubMed: 10634599]
35. Medeiros FA, Jammal AA. Validation of Rates of Mean Deviation Change as Clinically Relevant Endpoints for Glaucoma Progression. *Ophthalmology* 2022 Dec 24.

What is already known on this topic:

Optic disc photography is widely available and remains an important tool for the detection of glaucoma progression.

What this study adds:

An artificial intelligence algorithm can be leveraged to identify future glaucoma progression based on longitudinal series of optic disc photographs.

How this study might affect research, practice or policy:

The newly designed algorithm could help detect patients at high risk of functional glaucoma progression in the clinical setting once validated.

Synopsis:

We designed a deep-learning model to predict future functional glaucoma progression from longitudinal disc photographs. The model demonstrates high performance for predicting subsequent visual field progression and performed better in fast-progressing eyes.

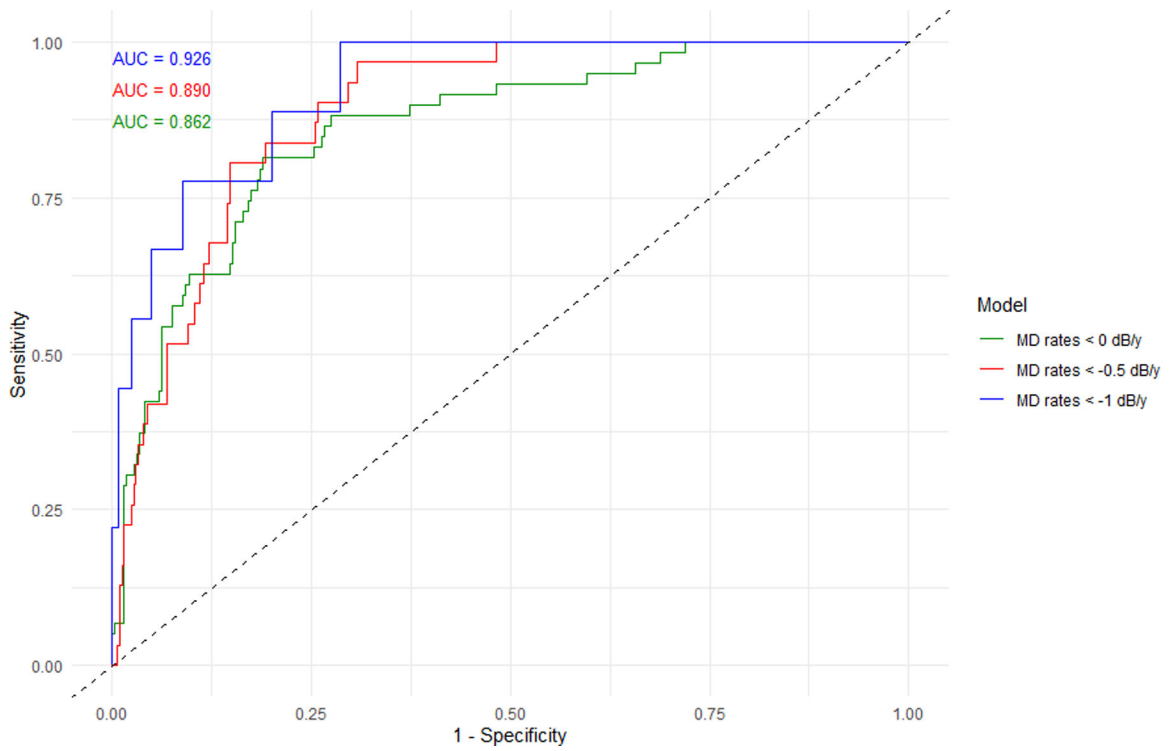


Figure 1. The receiver operating characteristic (ROC) curves for the prediction of functional glaucoma progression from a series of optic disc photographs with a deep learning model. The three curves represent the three sets of criteria used to define visual field progression during followup. The most stringent criterion for glaucoma progression (mean deviation (MD) rates of change <-1 dB/year) led to the highest area under the ROC curve (AUC) followed by MD rates <-0.5 dB/year and MD rates <0 dB/year criteria. None of the pairwise differences in AUCs was statistically significant.

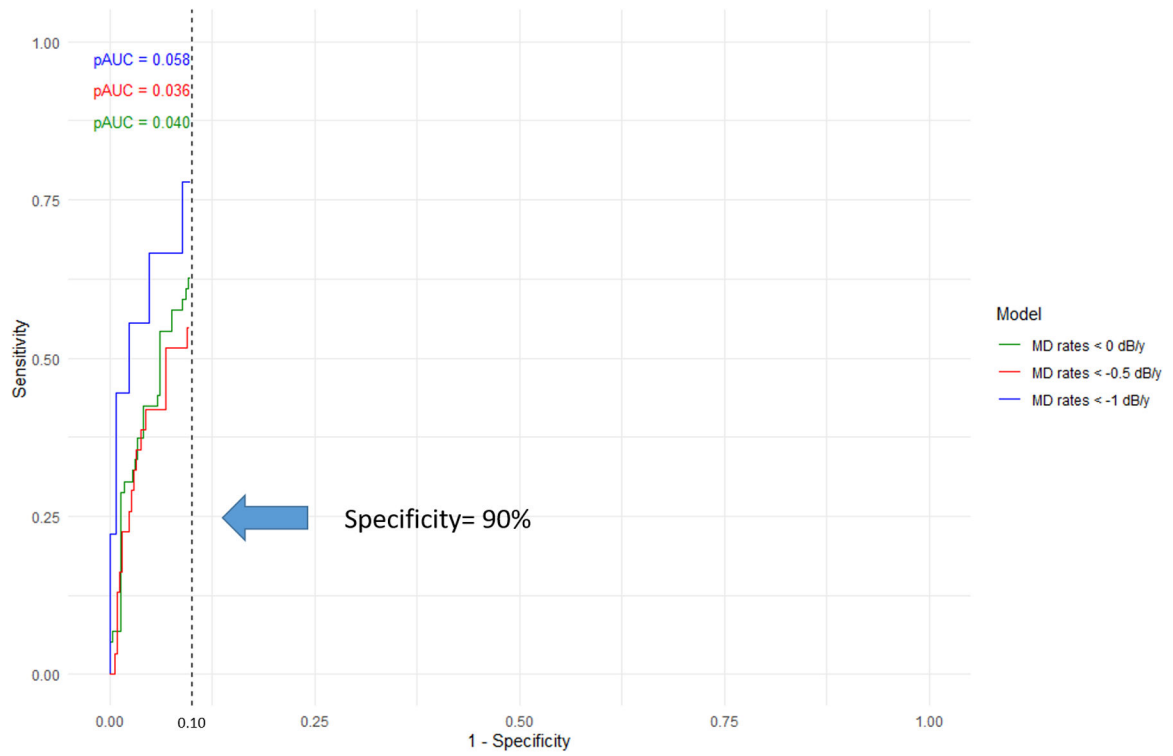


Figure 2. The partial area under receiver operating characteristic curves (pAUC) for prediction of functional glaucoma progression. The curves are presented for the model using criteria of mean deviation (MD) rates < 0 dB/year, < -0.5 dB/year and < -1 dB/year. The pAUCs were generated for a specificity of greater than 90%.

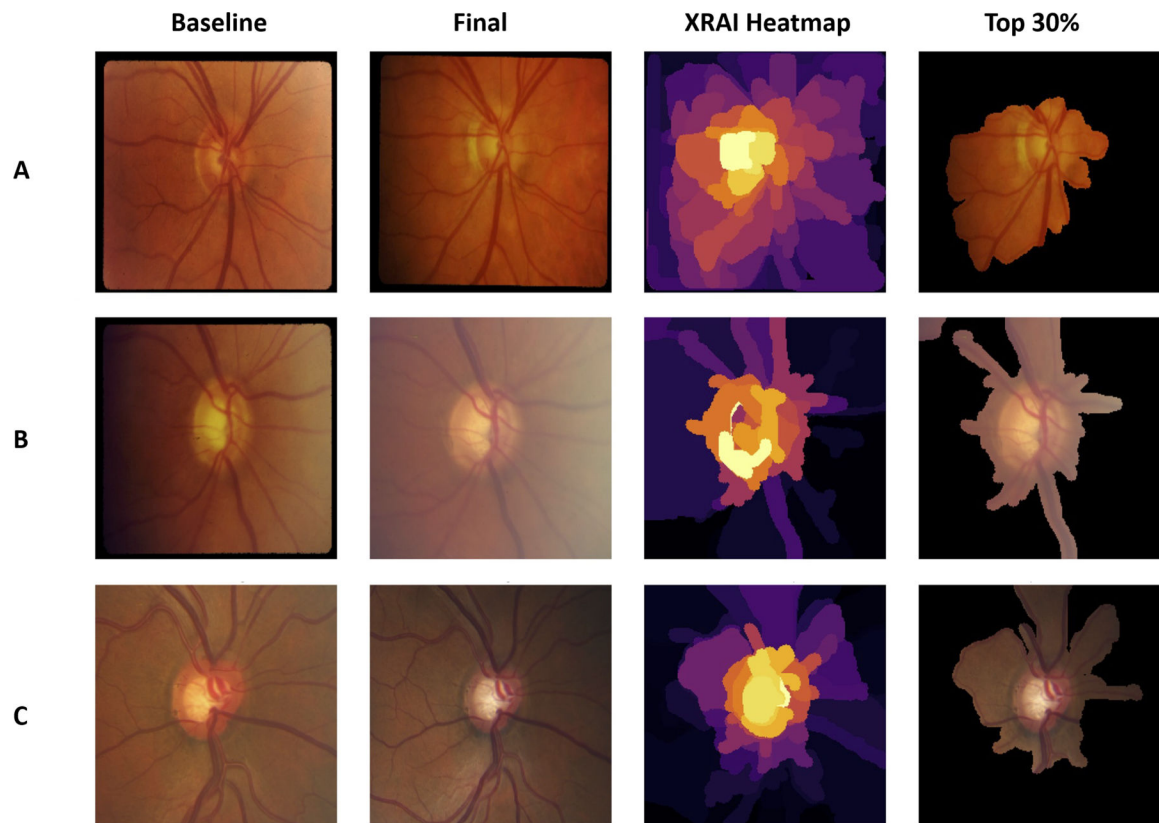


Figure 3. eXplanation with Ranked Area Integrals (XRAI) saliency plots for progressing and stable glaucoma eyes based on visual field findings. (A) An example of an eye with progressive generalised rim loss; (B) an example of an eye with progressive focal notching most prominent inferiorly; and (C) an example of a stable eye. The XRAI heat map (third column from left) demonstrates which regions of the final image have the most predictive power, that is, provide the most information. The most salient portion of the final image (the unmasked area) at an area threshold of 30% (fourth column from left) shows that in all the examples, the optic disc and the surrounding region correspond to the area with the most predictive power.

Table 1.

Demographic characteristics of the study participants.

| | Eyes = 3919, Patients = 2259 | | |
|--|-----------------------------------|--------------------------------------|---------|
| | Stable (Eyes = 3158, N = 1842) | Progressing (Eyes = 761, N = 417) | p value |
| <i>Age at baseline (years)</i> <i>Mean (SD)</i> | 59.5 (12.9) | 61.0 (11.4) | .001 |
| <i>Gender, number (percentage)</i> | | | |
| <i>Female</i> | 1015 (55%) | 246 (59%) | .31 |
| <i>Male</i> | 760 (41%) | 162 (39%) | .23 |
| <i>Unknown</i> | 62 (4%) | 9 (2%) | .15 |
| <i>Race, number (percentage)</i> | | | |
| <i>White</i> | 1067 (58%) | 250 (60%) | .62 |
| <i>African American</i> | 142 (8%) | 30 (7%) | .67 |
| <i>Asian</i> | 225 (12%) | 53 (13%) | .66 |
| <i>Hispanic</i> | 94 (5%) | 23 (6%) | .63 |
| <i>Unknown</i> | 309 (17%) | 61 (14%) | .78 |
| <i>Follow-up time (years)</i> <i>Mean (SD)</i> | 7.6 (4.7) | 10.3 (4.9) | < .001 |
| <i>Baseline mean deviation (dB)</i> <i>Mean (SD)</i> | -3.3 (4.9) | -3.6 (4.8) | .19 |
| <i>Number of visual field exams</i> <i>Median (IQR)</i> | 8 (6-12) | 13 (9-19) | < .001 |

SD = standard deviation; IQR = inter-quantile range

Table 2.

Performance of the deep learning model for prediction of subsequent visual field progression one or more year later using longitudinal pairs of optic disc photographs. The results are provided for the three criteria used for defining glaucoma progression (confirmed and significant MD rates <0 dB/year, <-0.5 dB/year and < -1.0 dB/year). Numbers in parentheses represent the 95% confidence intervals.

| Criteria | AUC | Sensitivity | Specificity | Accuracy |
|------------------------|------------------------|------------------------|------------------------|------------------------|
| MD rates <0 dB/year | 0.862 (0.812–0.913) | 83.0% (73.4%–91.4%) | 78.5% (68.8%–86.6%) | 80.0% (73.9%–84.6%) |
| MD rates <-0.5 dB/year | 0.890 (0.845–0.935) | 93.5% (77.4%–100%) | 77.5% (65.9%–88.4%) | 79.0% (68.5%–88.3%) |
| MD rates <-1.0 dB/year | 0.926 (0.857–0.994) | 100% (77.7%–100%) | 80.0% (67.9%–97.8%) | 80.4% (68.6%–97.4%) |

MD = mean deviation; AUC = area under ROC curve